

# AUTOMATIC 3D CHANGE DETECTION BASED ON OPTICAL SATELLITE STEREO IMAGERY

J. Tian, H. Chaabouni-Chouayakh, P. Reinartz, T. Krauß, P. d'Angelo

German Aerospace Center (DLR), Remote Sensing Technology Institute, 82234 Wessling, Germany –  
(Jiaojiao.Tian, Houda.Chaabouni, Peter.Reinartz, Thomas.Krauss, Pablo.Angelo)@dlr.de

**KEY WORDS:** Optical Stereo Data, DSM, Change Detection, Building, 3D-Analysis

## ABSTRACT:

When monitoring urban areas from space, change detection based on satellite images is one of the most heavily investigated topics. In the case of monitoring change in 2D, one major shortcoming consists in the lack of height change detection. Thereby only changes related to reflectance values or local textures changes can be detected. However, changes in the vertical direction are completely ignored. In this paper we present a new 3D change detection approach. We focus our work on the detection of changes using Digital Surface Models (DSMs) which are generated from stereo imagery acquired at two different epochs. The so called “difference image” method is adopted in this framework where the final DSM is subtracted from the initial one to get the height difference. Our approach is a two-step approach. While in the first step, reduction of the noise effects (coming from registration noise, matching artifacts caused by the DEM generation procedures, etc), the second one exploits the rectangular property of the building shape in order to provide an accurate urban area monitoring change map. The method is tested, evaluated and compared with manually extraction results over the city centre of Munich in Germany

## 1. INTRODUCTION

Change detection using automated image processing methods is a very important topic in satellite image processing. Numerous detection methods using various image types have been developed to satisfy a wide range of applications and user requirements (e.g. Singh 1989, Bruzzone 1997, Lu 2004). One major problem often met when restricting the change detection to the 2D information extracted from satellite images, is the lack of monitoring height changes, the 3D component of the surface to be analyzed. Thereby only changes related to the reflectance values and/or local textural changes are detected. However, changes in the vertical direction, such as building height changes are completely ignored. Such information could play an important role in different applications such as disaster assessment and urban area construction and/or destruction monitoring. Moreover, with the increasing availability of high resolution stereo imagery acquisition as well as the steady development of automatic DSM generation techniques (Zhang, 2005; Krauß, 2007; Akca, 2007; d'Angelo, 2008), comparison of the higher resolution DSMs acquired at different epochs on a same urban area should provide valuable information about the potential changes that have occurred at higher levels (e.g. building construction/destruction).

In the literature, several studies have been dedicated to the detection of changes using DSMs generated from stereo imagery. They can mainly be divided into two categories. The first change detection method is based on the joint-use of stereo and multi-spectral images (when they are available) and the generated DSMs are used in order to detect the changes that occur in the 2D space (spatial changes) as well as in the 3D space (height changes). In fact, the DSMs do not include spectral or textural information which could be of

great help when the task is to perform an accurate change monitoring. For example, Sasagawa (Sasagawa, 2008) integrated the DSM-difference map with the multispectral satellite images as an input to manual interpretation. Krauß (2007) applied a vegetation mask derived from multispectral data to the DSMs in order to concentrate only on urban structure changes. The second change detection method is based on DSM difference (when stereo or multispectral data is not available like in the case of Laser DSMs). The changed areas are detected through a simple subtraction of one DSM from another. This approach has been used in several researches (Zhang, 2005; Reinartz, 2006; Akca, 2007) for DSM precision assessment tasks. However, in this category of 3D change detection, the quality of the generated DSMs is quite determining regarding the accuracy of the final change maps. In fact, miss-coreregistrations and significant height differences that may arise between DSMs generated from different sources often results in the detection of virtual or irrelevant changes. In the work of Chaabouni-Chouayakh (2010) for example, post-processing steps such as morphological operations and contextual knowledge introduction have been proposed to remove virtual changes and to keep only the real ones.

In this paper, we focus on the detection of urban area changes (building construction/destruction). Our work includes vertical change as well as horizontal change. In this paper, the vertical change means the changes in height direction, while horizontal changes mentions the changes in planimetric direction, especially to detect the changing size of the subject in  $x$  and  $y$ . For the vertical changes, we compute the so-called “difference image” (Singh, 1989; Fung, 1990; Bruzzone, 2000) between two DSMs acquired over the city centre of Munich between 2003 and 2005. We adopt the robust image differencing method to eliminate the noise edges. After that,

different approaches have been adopted to highlight the real horizontal and vertical changes. For the horizontal changes, we apply an edge detection approach followed by a box-fitting method in order to extract the real changes relative to the constructed/destroyed building borders and remove the virtual ones coming from the different nature of the used DSMs. In the case of the vertical changes, we extract the height values of the changed objects based on a statistical method. Finally, the detection results are compared with the manual extraction records.

## 2. APPROACH TO THE 3D CHANGE DETECTION

### 2.1 Workflow of the proposed 3D change detection

We aim at extracting height information from the stereo imagery, then generating a change-detection map that represents 3D changes between the two datasets. We focus our research on noise reduction and change detection areas extraction.

The overall workflow of the proposed 3D change detection method is shown in Figure 1. The first step consists in generating DSMs from two pairs of registered optical stereo imagery acquired over the same area (here the city centre of Munich) at two different epochs  $t_1$  and  $t_2$ . In this paper, the DSMs are computed using the Semi-Global Matching (SGM) method (Hirschmüller 2008, d’Angelo 2008). A further co-registration between the two resulting DSMs has been necessary to remove any shift in three dimensions that might exist between the two DSMs. After that, the “difference image” is produced where real changes are highlighted and the influence of the noise (or virtual changes) is reduced (sub-section 2.2). Then, this difference image is analyzed by means of building edge detection in order to retrieve the borders of the different constructed/destroyed buildings. Both of the positive change (new constructed buildings) and negative changes (destroyed places) in vertical and horizontal direction are extracted.

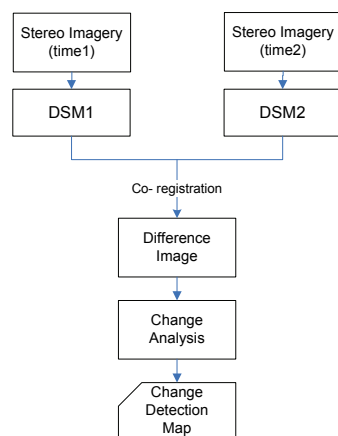


Figure 1. 3D Change detection process proposed in this paper.

### 2.2 Noise reduction

A major problem to cope with during change detection is the reduction of different kinds of noise. In our research, the noise is defined caused from: 1) Mis-coregistration. In practice, when two images are co-registered at sub-pixel accuracy, the true location of a pixel’s central point may be

anywhere within the pixels surrounding the point (Goodchild et al., 1994, Guillermo et al., 2009). It is unlikely that the footprints of two coincident pixels of the DSMs correspond to the same area (Bruzzone et al., 2003). 2) Quality of the DSM. Due to the erratic variations of the stereo images acquisition conditions, the DSM that generated from stereo imagery has some missing information (called holes in the DSM) caused by the unsuccessful stereo image matching of corresponding pixels. If we analyse the DEM from the pixel level in the change detection procedure, the “holes” will be detected and displayed as noise in the difference image. Many noise reduction methods have been developed in the literature (e.g. Gong et al., 1992; Bruzzone et al., 2003; Im et al., 2005 and Guillermo et al., 2009). In this research, we assume that each pixel in the first DSM shows the least difference with its true corresponding pixel in the second DSM. Therefore, we have chosen the “robust image differencing” method proposed in the work of Guillermo (2009). The robust difference between the initial DSM  $x_1$  and the final DSM  $x_2$  for the pixel  $(i, j)$ , is defined as the minimum of differences computed between the pixel  $x_2(i, j)$  in the final DSM and a certain neighbourhood (with size  $2*w+1$ ) of the pixel  $x_1(i, j)$  in the second DSM  $x_1$ . In mathematical words, the robust positive and negative differences  $X_{Pdif}(i, j)$  and  $X_{Ndif}(i, j)$  relative to the pixel  $(i, j)$  are defined as written in equations (1) and (2), respectively:

$$X_{Pdif}(i, j) = \min_{(p \in [i-w, i+w], q \in [j-w, j+w])} \{(x_2(i, j) - x_1(p, q)) > 0\} \quad (1)$$

$$X_{Ndif}(i, j) = \max_{(p \in [i-w, i+w], q \in [j-w, j+w])} \{(x_2(i, j) - x_1(p, q)) < 0\} \quad (2)$$

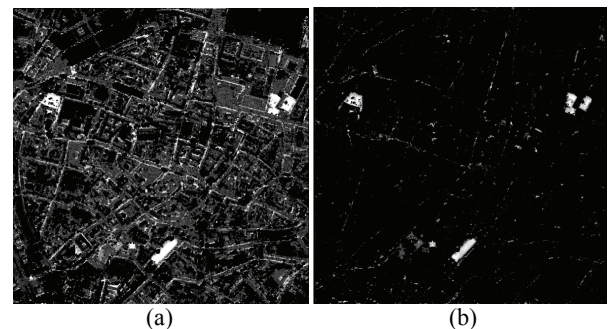


Figure 2. Noise reducing procedure: (a) Original image difference result; (b) Robust image difference result.

Figure 2 shows a comparison between a simple pixel-to-pixel difference between the DEMs and a robust DEM difference. In Figure 2 (a), although the changed areas are highlighted to some extent, the background is very noisy, which will be a problem in the change information extraction procedure. In contrast, after executing the robust image difference in Figure 2 (b), the noise in the background is successfully reduced, while the white areas, which are more likely to be real changed areas, are not influenced significantly.

### 2.3 Change areas extraction

In binary change detections, one of the most important final steps consists in highlighting real positive and negative changes. For spectral images, a simple thresholding of the histogram has been widely used to stress real changes and remove the virtual ones (Bazi, 2005; Bovolo, 2006; Sen and Pal, 2009). While for the 3D change detection, in the DSM generation procedure, much information is already missing. Simple thresholding on the “difference image” will destroy the more original information. Therefore, automatic building extraction approach is adopted in our research. It can be divided into 3 steps,

- 1) Edges extraction: In this step, the Canny edge (Canny, 1986) extraction method has been adopted. As our focus in this work consists in the detection of the urban changed man-made structures (building construction/destruction), small edges will not be considered in our research.
- 2) Mask generation: Since most of the Canny edges are open, and could not be filled automatically, we choose to close all of the edges with morphological algorithms. We fill each closed edge to single mask, which presents the changed area.
- 3) Box-fitting based building shape refinement: In general, according to the quality of the original DSM data and also the edge detection and mask filling result, most of the edges are highly curved and much information is missed. Therefore, the building edges need to be refined so that they regain their sharp shapes. In this work, we used the box-fitting method proposed by (Sirmacek and Unsalan, 2008). For this method, we need seed points, which show the location of the changed building; the edges which control the size of the box for the changed building; and also the automatic box growing direction and stop condition. In our research, we locate the seed points in the centre of each mask that is generated in step 2. Only the original edges around each buffered mask area are considered to be the edge of this building.

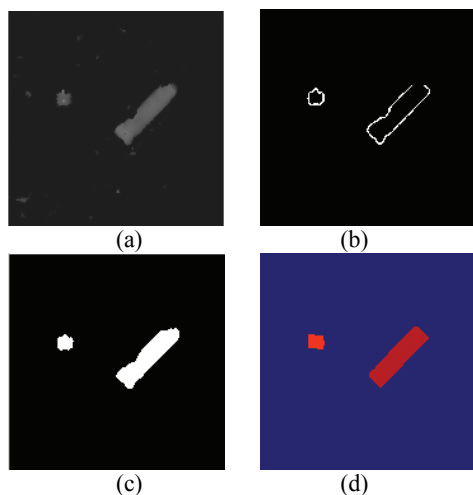


Figure 3. Change areas extraction: (a) Robust difference image; (b) Edges extraction; (c) Changed building masks generation; (d) Box-fitting-based shape refinement of the changed areas.

Figure 3 summarizes the results of the already described steps when applying our changed areas extraction on a subset from

the original difference image of Figure 2 (b) that is depicted in Figure 3 (a). Figure 3 (b) shows the edges extraction results where only important edges are kept (small edges are removed). The mask generation output is displayed in Figure 3(c). The result of the box-fitting method is depicted in Figure 3 (d) where a more refined version of the changed objects is obtained.

In the change value extraction procedure, the horizontal change can be easily calculated according to the pixel numbers of the mask area and the DSM resolution. In order to get only one vertical change value  $C_i$  for each constructed/destroyed building defined by  $Mask_i$  or box-fitting result. We average the pixels values in the “difference image” belonging to the same changed object, and define this value as the vertical change of each building. In the following, we exclude all pixels, which have ‘0’ value (no height in the changed area), very low values or very high values and could therefore be artifact change, so that these pixels will not be involved in the mean value calculation procedure. As displayed in Figure 4, only the middle part (gray colour filled) of the height difference values are used.

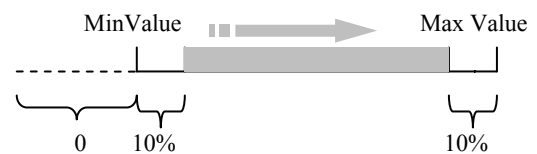


Figure 4. Vertical change value extraction strategy.

## 3. EXPERIMENTAL RESULTS

### 3.1 Description of the data

In order to evaluate the performance of our approach, we have chosen the city centre of Munich in Germany as study site. Two DSMs from two different epochs have been used to detect the potential changes. The first DSM (called in the following as IKONOS-DSM) is computed from IKONOS in-orbit stereo imagery (level 1A, viewing angles  $+9.25^\circ$  and  $-4.45^\circ$ ) with one meter spatial resolution, acquired in July 2005. It has been generated using the Semi Global Matching (SGM) algorithm implemented at DLR (d’Angelo, 2009). Due to the lack of another stereo pair, the second one we use instead a DSM which is generated from a LiDAR point cloud data acquired in February 2003 (called in the following as LiDAR-DSM).

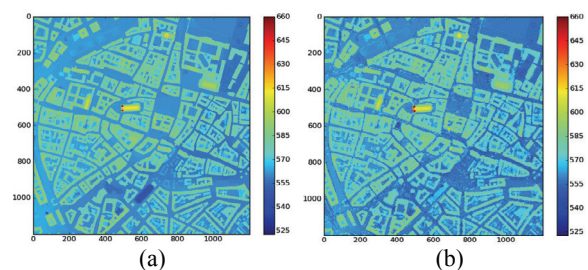


Figure 5. DSMs of the city centre of Munich: (a) LiDAR-DSM (2003); (b) IKONOS-DSM (2005), vegetation cover removed.

Since the LiDAR data used in this work is generated from the last return pulses, which represent the bare earth terrain, the vegetation cover information is almost fully removed.

Therefore, changes at the vegetation level could not be detected. In order to focus on the urban changes, a vegetation mask, computed from the IKONOS multispectral data, has been used. This mask has been generated using the Normalized Differenced Vegetation Index (NDVI). Figure 5 displays the two DSMs used in this article after removing of the vegetation area applying the vegetation mask.

### 3.2 Generation of the difference image.

Following the procedure described in subsection 2.2, after the co-registration of the two DSMs depicted in Figure 5, we apply the “robust difference” approach to calculate the difference images, where noise has been reduced and changes can be better analyzed. As we can see from Figure 5, in the LiDAR-DSM, the building edges are sharper than in the IKONOS-DSM. Therefore, we choose a  $7 \times 7$  window ( $w=3$  in equations (1) and (2)) in the noise reduction procedure for this evaluation.

Both the positive (which highlights the new constructed areas) and negative difference image (which highlights the destroyed areas) were generated in this step. Figure 6(a) displays the positive robust image difference obtained when applying a  $7 \times 7$  window in the noise reduction step. The dark blue colour means no change, and the light blue colour corresponds to height changes of about 20 meters.

### 3.3 3D change detection maps

The different steps of the proposed 3D change detection method applied to the city centre of Munich are displayed in Figure 6. Figures 6 (a-c) present the positive change results. The positive difference image is displayed in Figure 6 (a). The corresponding change mask is shown in figure 6 (b). Figure 6 (c) depicts the final change detection map, under the assumption that each building has only one height value, computed as described in subsection 2.3. As can be seen from the change detection results, 6 new buildings are detected. The buildings No.4 and 5 are detected as one building in the mask map (showed in figure 6(b)), due to errors in the DSM generation procedure. To separate the two buildings, in the box-fitting procedure, we extract two seed points in this area based on image eroding result. And we use the original edges in the box growing procedure, so the image eroding will not influence the accuracy of the result.

The same steps have been adopted to detect the negative changes (presented in figures 6 (d-f)). According to the negative change detection results, four building masks are detected. But three of them are in strange shape, with relative low height values. Also, the box-fitting procedure fails in

fitting these buildings to regular rectangular shape. This suggests them to be false alarms (as shown in Table 1). Therefore, only one building is remaining in the negative change map.

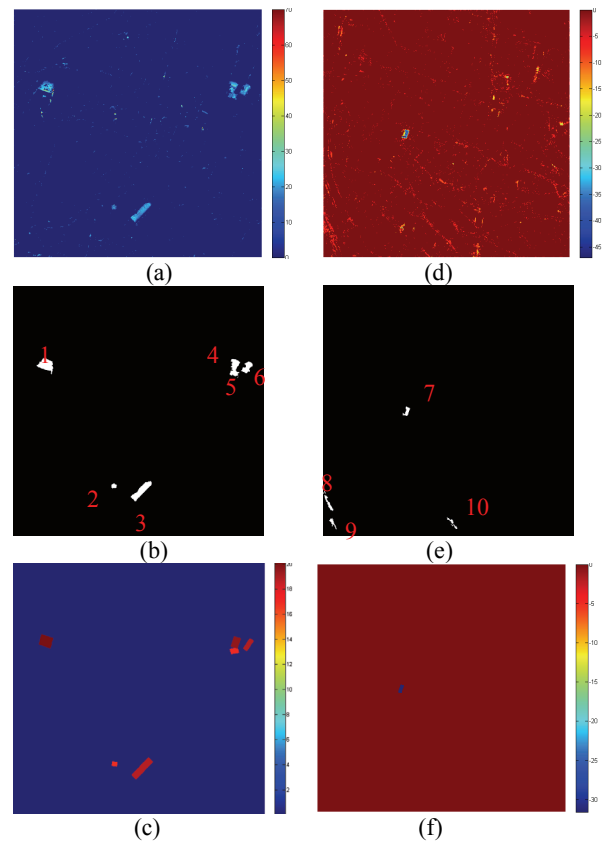


Figure 6. Change detection results: (a) Positive difference map; (b) Positive change mask; (c) positive change map; (d) Negative difference map; (e) Negative change mask; (f) Negative change map

## 4. RESULTS AND DISCUSSION

In order to allow a quantitative evaluation of the effectiveness of the presented methods, and also to study the influence of the building shapes on the change extraction procedure, we compare the mask-based change maps to the box-fitting based ones. A manually annotated change map has also been included in the evaluation scheme:

Table 1. Change Detection Result Comparison

| No. | Change Type     | Mask-Based |                        | Box-fitting Based |                        |      |            | Manual Extraction      |       |      |      |
|-----|-----------------|------------|------------------------|-------------------|------------------------|------|------------|------------------------|-------|------|------|
|     |                 | Height [m] | Area [m <sup>2</sup> ] | Height [m]        | Area [m <sup>2</sup> ] |      | Height [m] | Area [m <sup>2</sup> ] |       |      |      |
| 1   | Positive change | 19.58      | 3247                   | 19.80             | 3077                   |      | 22.0       | 2788                   |       |      |      |
| 2   | Positive change | 19.10      | 491                    | 16.46             | 576                    |      | 17.00      | 465                    |       |      |      |
| 3   | Positive change | 18.97      | 3344                   | 19.10             | 3748                   |      | 18.8       | 3694                   |       |      |      |
| 4   | Positive change | 18.78      | 2553                   | 19.55             | 18.26                  | 1818 | 2911       | 19.2                   | 17.90 | 1377 | 2289 |
| 5   | Positive change |            |                        | 16.97             |                        | 1093 |            | 16.6                   |       | 912  |      |
| 6   | Positive change | 18.64      | 1683                   | 18.69             | 1409                   |      | 20.2       | 945                    |       |      |      |
| 7   | Negative change | -33.72     | 762                    | -32.42            | 800                    |      | -36.0      | 1007                   |       |      |      |
| 8   | Negative change | -6.2       | 1044                   | ----              | ----                   |      | ----       | ----                   |       |      |      |
| 9   | Negative change | -6.43      | 578                    | ----              | ----                   |      | ----       | ----                   |       |      |      |
| 10  | Negative change | -6.30      | 565                    | ----              | ----                   |      | ----       | ----                   |       |      |      |

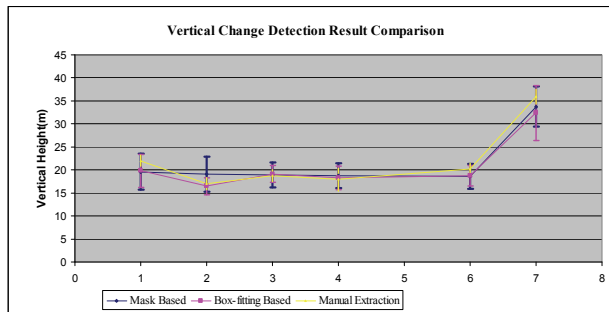


Figure 7. Vertical Change Detection Result Comparison

- For the annotation of the horizontal changes (areas of the changed objects), the areas of the positive (resp. negative) changed objects have been manually extracted using the original IKONOS panchromatic channel (resp. using the LIDAR DSM data).
- For the annotation of the vertical changes (height of the changed objects), we extract the height value in the changed area from each DSM manually, and calculate the difference.

The final change detection results are summarized in Table 1. To compare the two automatic detection result and manual extraction result, we show the vertical and horizontal change extraction result separately in Figures 7 and 8 (For the negative changes, we use the absolute values in Figure 7). As the 4<sup>th</sup> and 5<sup>th</sup> changes could not be separated in the detected mask, we consider them as one changed object in the comparison procedure. Also false alarms are omitted in our comparison scheme. According to the error bars (get from the standard deviation of the height value distribution in the mask area), the detected vertical changes fit well with the manual extraction result. For the 1<sup>st</sup> building, the manual extraction result shows relatively larger difference with both the mask based and box-fitting based automatic extraction result. In order to explain such behaviour, we compare the generated DSMs to the IKONOS panchromatic image. As showed in Figure 9, the IKONOS-DSM in this area has poor quality, resulting in 3 big holes in the middle of the building, and the building shape is strongly transformed. This explains well the large height difference found between our change maps and the manual extraction one.

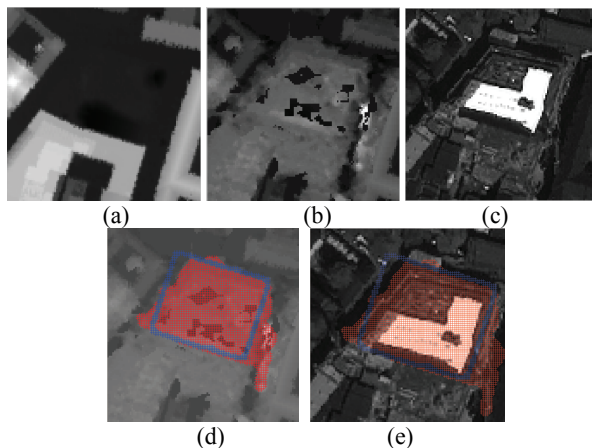
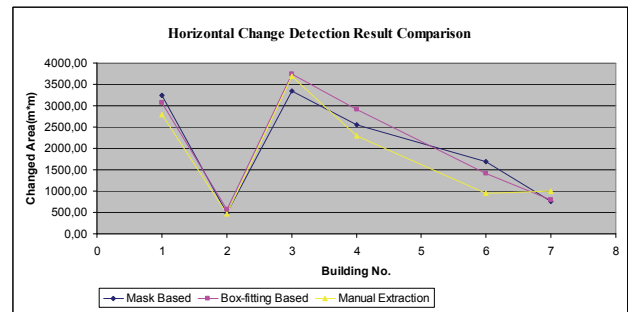
Figure 9. 1<sup>st</sup> changed building analysis: (a) LiDAR-DSM; (b) IKONOS-DSM; (c) IKONOS-PAN-2005; (d) Mask with IKONOS-DSM; (e) Masks with the IKONOS-PAN-2005

Figure 8. Horizontal Change Detection Result Comparison

In the Figure 9 (d-e), the red mask represents the masked shape, while the blue rectangle is the extracted change building shape after box-fitting. We can see that the mask fits well with the building area in IKONOS-DSM, but has quite large difference with IKONOS-PAN-2005, after the box-fitting, the right parts of the outliers are successfully recovered. But the result is limited by the rectangular shape assumed in the box-fitting procedure, which displayed by the false alarm pixels in the left upper part inside the blue colour rectangle. Those situations conduct the relative lower vertical changes, while higher horizontal changes in the extraction results.

## 5. CONCLUSION

In this paper, a 3D change detection approach based on DSMs is proposed and evaluated to detect changes that have occurred in the city centre of Munich between 2003 and 2005.

The whole procedure is divided into 3 steps. First, we generate and co-register DSMs acquired at two different epochs. Then, we compute the “robust difference images” in order to reduce the noise coming from the different nature of the DSMs used. In fact, the random variations of the stereo images acquisition conditions as well as the blunders caused during the automatic matching and DEM generation process makes urban structures look different from one DSM to another, especially for building walls and edges. As our focus in this paper is the monitoring of urban changes, noise reduction is essential. After that, we generate the change map with both vertical and horizontal change information. To overcome the poor quality of the DSM, we refine the changed buildings to rectangular shape. To confirm the validity of our approach, we compare our results with manual extracted ground truth figures.

It has been shown that DSMs generated from optical stereo imagery could be reliable sources for efficient 3D change detection. The extracted change maps demonstrate the ground surface changes in most parts of the test areas. But when the DSM does not meet the required quality and can not show the real situation, the result will be influenced. In addition, only rectangular building shapes have been considered in our refinement procedure, the change results will certainly improve when more building shapes are included.

## ACKNOWLEDGEMENTS

The authors wish to thank Beril Sirmacek for contributing her box-fitting algorithm, and Hossein Arefi for his advice in the pre-processing of the DSM.

## REFERENCES

- Akca, D., 2007. Least Squares 3D surface matching. Ph.D. thesis, *Institute of Geodesy and Photogrammetry*, ETH Zurich, Switzerland
- Bazi, Y., Bruzzone, L., and Melgani, F., 2005. An Unsupervised Approach Based on the Generalized Gaussian Model to Automatic Change Detection in Multitemporal SAR Images, *IEEE Transactions on Geoscience and Remote Sensing*, Vol. 35, No. 4, July 1997
- Bovolo, F., 2006. Advance Methods for Automatic Change Detection in Multitemporal Remote Sensing Images Acquired by SAR and Multispectral Sensors, *PhD Dissertation*, University of Trento. December 2006
- Bruzzone, L., and Serpico, S.B., 1997. An Iterative Technique for the Detection of Land-Cover Transitions in Multitemporal Remote-Sensing Images, *IEEE Transactions on Geoscience and Remote Sensing*, Vol. 35, No. 4, July 1997
- Bruzzone, L., and Prieto, D.F., 2000. Automatic Analysis of the Difference Image for Unsupervised Change Detection. *IEEE Transactions on Geoscience and Remote Sensing*, Vol. 38, No. 3, May 2000
- Bruzzone, L., and Cossu, R., 2003, An Adaptive Approach to Reducing Registration Noise Effects in Unsupervised Change Detection. *IEEE Transactions on Geoscience and Remote Sensing*, Vol. 41, No. 11, November 2003
- Canny, J., 1986. A computational approach to edge detection. *IEEE Transactions on Pattern Analysis and Machine Intelligence*, 8 (6), pp. 679-698
- Castilla, G., Guthrie, R. , and Hay, G.J., 2009. The Land-cover Change Mapper(LCM) and its Application to Timber Harvest Monitoring in Western Canada, *Photogrammetric Engineering & Remote Sensing, Special Issue on Change Analysis*, Vol. 75, No. 8, August 2009
- Chaabouni-Chouayakh, H., Krauss, T., d'Angelo, P., and Reinartz, P., 2010. 3D Change Detection inside Urban Areas using different Digital Surface Models, *ISPRS International Archives of the Photogrammetry, Remote Sensing and Spatial Information Sciences*, Vol. 39 (3), Accepted
- Choi, K., Lee, I., and Kim, S., 2009. A feature based approach to automatic change detection from lidar data in urban areas, *ISPRS Workshop Laserscanning 2009*, Paris, France
- d'Angelo, P., Lehner, M., and Krauss, T., 2008. Towards Automated DEM Generation from High Resolution Stereo Satellite Images, *International Society for Photogrammetry and Remote Sensing*, pp. 1137-1342
- Fung, T., An Assessment of TM Imagery for Land-cover Change Detection, *IEEE Transactions on Geoscience and Remote Sensing*, Vol. 28, No. 12, 1990
- Goodchild, M.F., 1994. Integrating GIS and Remote Sensing for Vegetation Analysis and Modelling: Methodological Issues. *Journal of Vegetation Science*, 13 (4), pp 773-779
- Hirschmüller, H., 2008. Stereo processing by semiglobal matching and mutual information. *IEEE Transactions on Pattern Analysis and Machine Intelligence*, 30 (2), Feb. 2008.
- Krauß, T., Reinartz, P., and Stilla, U., 2007, Extracting Orthogonal Building Objects in Urban Areas From High Resolution Stereo Satellite Image Pairs, *International Archives of Photogrammetry, Remote Sensing and Spatial Information Sciences*, 36(3/W49B)
- Murakami, H., 1999, Change Detection of Buildings Using an Airborne Laser Scanner, *ISPRS Journal of Photogrammetry & Remote Sensing*, Vol. 54, pp.148-152.
- Lu, D., Mausel, P., Brondizio, E. & Moran, E., 2004, Change Detection Techniques. *International Journal of Remote Sensing*, 25 (12), pp 2365-2407.
- Reinartz, P., Müller, R., Lehner, M., and Schroeder, M., 2006. Accuracy Analysis for DSM and Orthoimage Derived from SPOT HRS Stereo Data Using Direct Georeferencing. *ISPRS Journal of Photogrammetry and Remote Sensing*, Vol. 60, No. 3, pp 160-169
- Singh, A., 1989, Digital change detection techniques using remotely-sensed data. *International Journal of Remote Sensing*, 10 (6), pp 989-1003
- Sirmacek, B., and Unsalan, C., 2008, Building Detection From Aerial Imagery using Invariant Color Features and Shadow Information. In *Proceeding of International Symposium on Computer and Information Science (ISCIS)*, 1, pp 1-5
- Zhang, L., 2005, Automatic Digital Surface Model (DSM) Generation from Linear Array Images. Ph.D. Thesis, *Institute of Geodesy and Photogrammetry*, ETH Zurich, Switzerland